

Modern Random Access: an Age of Information Perspective on Irregular Repetition Slotted ALOHA

Andrea Munari, *Senior Member, IEEE*

Institute of Communications and Navigation, German Aerospace Center (DLR), 82234 Wessling, Germany

Email: {Andrea.Munari}@dlr.de

Abstract

Recent years have witnessed a steadily growing interest towards *modern random access* protocols for massive machine type communications in next generation wireless systems. Constructively embracing interference, these solutions have been shown to attain a spectral efficiency comparable to that of coordinated access schemes, while remaining true to the grant-free paradigm. On the other hand, their ability to maintain a fresh and up-to-date view at the receiver when devices transmit status updates, as typical in IoT applications, is still largely unexplored. In this paper we start to bridge such a gap, focusing on a scenario in which a large population of devices share a common wireless channel in an uncoordinated fashion, and studying the age of information (AoI) metric when medium access follows the irregular repetition slotted ALOHA (IRSA) protocol. By means of a Markovian analysis, we track the AoI evolution for a source at the receiver, prove that the process is ergodic, and derive a compact closed form expression for its stationary distribution. Leaning on this, we compute exact formulations for the average AoI and for the peak-age violation probability. The study reveals non-trivial design trade-offs for IRSA, highlighting the key role played by the protocol operating frame size. Moreover, a comparison with the performance of a simpler slotted ALOHA strategy highlights a remarkable potential for modern random access in terms of information freshness.

Index Terms

age of information, grant-free access, irregular repetition slotted ALOHA, IoT, massive machine-type communications

The author would like to thank Gianluigi Liva and Giuseppe Durisi for the fruitful discussions on the topic.

I. INTRODUCTION

The relentless rise of internet of things (IoT) applications is calling for novel communications paradigms, which will define next generation wireless systems [1], [2]. Among the multiple challenges posed to all layers of the protocol stack, the need to provide connectivity to a vast population of often low-power, low-complexity devices is leading to profound design evolutions in terms of medium access control [3]. The traffic profile encountered in massive machine-type communications (mMTC), characterised by transmissions of short packets in a sporadic and unpredictable fashion, renders indeed traditional grant-based policies highly inefficient due to the excessive cost of overhead. This is the common case, for instance, of uncoordinated devices transmitting updates or sensors monitoring a physical quantity.

To effectively support such use cases, grant-free access protocols based on variations of the well-known ALOHA policy [4] have been proposed, and represent the de-facto approach for IoT in commercial solutions (e.g., LoRa [5], SigFox [6]) and standards (e.g., NB-IoT, LTE-M [7]) for both terrestrial and non-terrestrial networks [8]. Moreover, the need to support massive sets of devices has recently focused research efforts on the development of a new family of schemes, often labelled as *modern random access*, which smartly and constructively embrace interference – the bottleneck for ALOHA – to significantly boost performance. Following different strategies, see, e.g. [9], [10], [11], [12], [13], [14], [15], [16], these solutions have been proven to be competitive to their coordinated counterparts in terms of throughput and spectral efficiency, while remaining true to the grant-free paradigm. A relevant example is offered by irregular repetition slotted ALOHA (IRSA) [17], which foresees nodes independently transmit multiple copies of their packets over a frame of predefined length, and resorts to successive successive interference cancellation (SIC) to recover information at the receiver side. Thanks to its performance, and to the good level of maturity it reached, the scheme became part of the ETSI DVB-RCS2 standard for return-link satellite communications [18], stressing the potential of modern random access in supporting future developments of mMTC scenarios.

In parallel to the design of advanced grant-free protocols, the past few years have also witnessed a steadily growing interest towards the definition of novel performance metrics for IoT. When serving a large number of status reporting devices, in fact, the main goal is often to maintain a fresh and up-to-date view on the sources, e.g., to drive decisions or feedback loops. In such conditions, even a highly efficient utilisation of the shared medium that leads to delivery of

stale or scarcely relevant information would be highly suboptimal from an application standpoint. These remarks have triggered a florid line of study, aiming at the design of transmission policies based on the *semantic* of information [19], [20], [21]. The pioneering concept in the field has been that of age of information (AoI), originally formalised in [22], [23] in the context of vehicular communications. Specifically, the metric is defined focusing on the delivery of time-stamped messages of equal importance, and captures knowledge freshness at the receiver by measuring the time elapsed since the generation of the latest received update from a given source. Despite its simplicity, AoI pinpoints a fundamental performance tradeoff, as it depends both on the traffic generation pattern – more frequent messages offering fresher information –, and on the delivery latency experienced by transmissions within the network – higher traffic leading to larger delays and stronger jitters. In view of this, the metric provides insights that may depart significantly from classical throughput or latency optimisation criteria, and has been investigated in a number of setups [24]. From this viewpoint, a good level of maturity has been reached for point-to-point links, see, e.g. [25] and references therein, and interesting results are emerging in IoT setups where multiple devices share the same channel to report to a common destination. Among these, optimal scheduling policies are derived in [26] considering packets of different durations to be delivered over noisy channels, whereas joint sampling and orthogonal transmission strategies are studied in [27] and in [28] under energy constraints. Distributed and low-complexity scheduling solutions are proposed in [29] limiting the negotiation overhead, and in [30] meeting throughput requirements, whereas [31] tackles the behaviour of AoI under orthogonal and non-orthogonal multiple access. On the other hand, research has lately started to focus on models that deal with the additional degree of complexity introduced by having terminals share the channel in an uncoordinated fashion. Initial and key steps have been taken with the exact characterisation of the average AoI of slotted ALOHA (SA) [32], [33]. Both works pinpoint an inverse proportionality between information freshness and aggregate throughput, revealing how maximising the latter also leads to the minimum AoI under symmetric channel conditions and for the classical destructive collision model. In the presence of feedback, important improvements were unleashed in [34], which foresees devices tune their SA transmission probability based on the notion of age-gain, i.e., sending updates only when their impact on refreshing the receiver’s perception of the source’s state is strong enough. Recent works have also started to look into fully asynchronous random access, deriving AoI metrics for pure ALOHA [35] and carrier-sense based protocols [36].

Despite the lively research on the field, however, the performance of *modern random access* in terms of AoI is still largely unexplored, with the exception of [37], which derived the average AoI for IRSA. Taking the lead from this, the present paper sheds more light on the behaviour of advanced grant-free solutions for mMTC from an information freshness standpoint. Specifically, we focus once more on IRSA, and track the evolution of the instantaneous AoI for a source that shares a wireless channel with other contending nodes. Following this approach, we provide the following key and novel contributions:

- resorting to a Markovian analysis, we show that the process admits a stationary distribution, and characterise it with a compact closed-form expression. Leaning on this result, we provide a simpler and alternative derivation of the average AoI in accordance with [37]
- we then complement our work by studying the behaviour of the age distribution tail. Indeed, while average performance provides useful insights, exceeding a threshold value for the AoI may be of more relevance for some practical applications. This is the case, for instance, of dynamic system control, where decision making based on stale information may have dire consequences. To provide design guidance we thus focus on the metric of *peak age violation probability*, originally introduced in [38], for which we provide an exact closed-form expression
- the Markovian analysis is also applied to a SA-based system, leading to simple formulations for average AoI – in accordance with [32], [33] – and peak age violation probability. A thorough comparison between the performance achievable with the different grant-free access schemes highlights a strong potential for modern random access even in terms of AoI
- the presented framework reveals non-trivial trade-offs for IRSA, for which the closed-form derived expressions offer a simple yet powerful design tool. In particular, and in contrast to what known for SA, we show how tuning the system so as to achieve the maximum throughput is not the only driving force in determining AoI. From this angle, the critical role played by the frame duration is explored and discussed, identifying the best operating conditions for information freshness under different channel loads
- while the presented results are instantiated and discussed for IRSA, the analytical framework holds for a larger class of modern random access protocols, offering broadly applicable tools.

The remainder of the manuscript is organised as follows. We start our discussion in Sec. II

by introducing the system model considered throughout the discussion, and summarising the key features of the studied grant-free protocols. Starting from this, we derive analytically the behaviour in terms of average and peak age violation probability in Sec. III for both IRSA and SA. The performance of the schemes is compared via numerical results in Sec. IV, prior to drawing conclusions in Sec. V.

II. SYSTEM MODEL AND PRELIMINARIES

Let us focus on a system with n users sharing a wireless channel to attempt delivery of status updates towards a common receiver (or sink). Time is divided in slots of equal duration T_s , and all terminals are assumed to be synchronised to such pattern. Leaning on this, we measure for convenience all time-related quantities in (fraction of) slots, i.e. normalise them to T_s , and, for the sake of notation simplicity, we set without loss of generality $T_s = 1$.

At each time slot, every user may independently become active with probability ρ , generating a packet addressed to the sink and marked with a time-stamp that reports the start of the current slot. We shall assume all messages to be equally important, and are interested in having a system that collects and maintains an up-to-date picture of the status of each device. To this aim, we keep track of the *current age of information* for user i at the sink, defined as

$$\delta^{(i)}(t) := t - \sigma^{(i)}(t) \quad (1)$$

where $\sigma^{(i)}(t)$ denotes the time-stamp of the last received update from node i as of time t .¹ It is relevant to observe that the stochastic process $\delta^{(i)}(t)$ is driven both by the activation pattern of the devices and by the ability to timely deliver updates offered by the employed medium access policy. Specifically, the current AoI for a node grows linearly with time, being reset only when a time-stamped packet is decoded, and leading to a typical sawtooth profile exemplified, e.g., in Fig. 1. For our study, we focus in particular on the *average network AoI*

$$\Delta := \frac{1}{n} \sum_{i=1}^n \Delta^{(i)} \quad (2)$$

where $\Delta^{(i)}$ is the time average of the current AoI of the i -th node, i.e.

$$\Delta^{(i)} := \lim_{t \rightarrow \infty} \frac{1}{t} \int_0^t \delta^{(i)}(\tau) d\tau. \quad (3)$$

¹Consistently with the definition, also AoI related quantities are measured in (fraction) of slots, i.e. normalised to T_s .

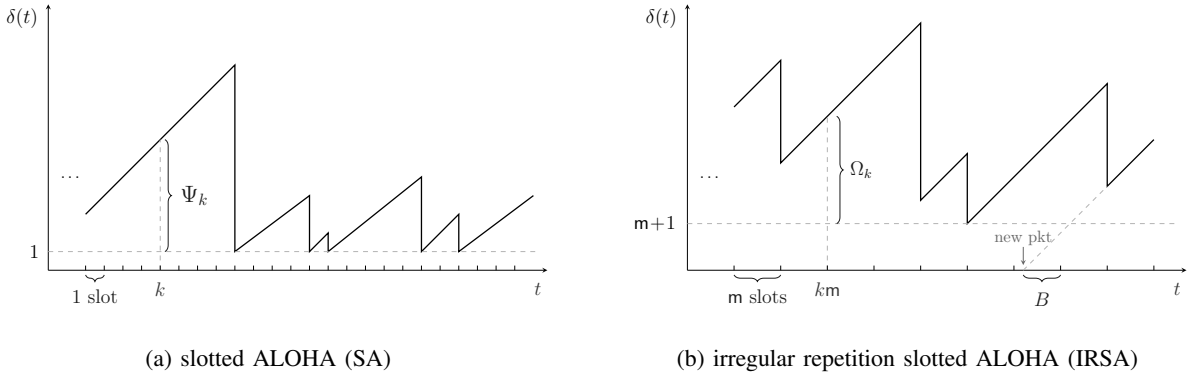


Fig. 1. Example of realisations for the current AoI $\delta(t)$ of a source when using SA (left), and IRSA (right). Ψ_k and Ω_k indicate the stochastic processes tracking current age of information in the two cases (see Sec. III).

Moreover, we are interested in the long term behaviour of the process, and evaluate the probability for the current AoI of a user to exceed a threshold value, as will be formally introduced in Sec. III with the notion of *peak age violation probability*.

With an eye on mMTC applications, we compare the performance of two grant-free access protocols: SA – taken as a reference benchmark in view of its widespread application –, and IRSA. Following a common and well established modelling assumption for slotted systems, e.g. [4], [10], we regard collisions as destructive, so that the superposition of two or more concurrent transmissions over the same slot prevents decoding at the receiver. On the other hand, a slot seeing the presence of a single packet always leads to retrieval of the information content. For both schemes, no feedback nor retransmission policies are considered, so that a packet is transmitted at most once.² Finally, to characterise the information freshness metrics, we will also refer to the aggregate throughput S of the system, defined as the average number of packets per slot decoded at the sink, upper bounded to 1 [pkt/slot] under the considered channel model.

A. Slotted ALOHA

Following the SA policy, a node accesses the channel to send an update as soon as this is generated. Accordingly, at every slot the device successfully delivers a packet to the sink with probability

$$\xi_{\text{sa}} := \rho(1 - \rho)^{n-1} \quad (4)$$

²We note that the lack of feedback is encountered in many mMTC applications, either to reduce downlink bandwidth consumption or to limit devices complexity and energy consumption.

where the first factor accounts for the node to become active, i.e., to have generated a new status update, while the latter for no other user to transmit concurrently, so to enable a successful message delivery. In this case, the current AoI for the device is reset to 1, as only the one-slot interval needed for packet transmission elapses from the generation of the update to its reception (see Fig. 1a). As all nodes operate independently, the number of successful deliveries per slot is a binomial r.v. of parameters (n, ξ_{sa}) , whose expected value gives the aggregate throughput of the scheme

$$S_{sa} = n\rho(1 - \rho)^{n-1}.$$

B. Irregular repetition slotted ALOHA

Under IRSA operations [17], access to the medium is organised in frames of duration m slots each. Users are frame-synchronous, and the first transmission opportunity for a new packet is granted only at the start of the next frame. With the traffic generation pattern of our system, this implies that a node may become active more than once before being able to access the medium. Aiming to provide the sink with the most up-to-date information, we assume a device in such a situation to transmit the last generated update only, discarding all the others.³

A terminal that has become active at least once during an m -slot period will then initiate a transmission at the start of the subsequent frame. In this case, the node sends ℓ identical replicas of its update, uniformly placed at random over the m available slots. The number of copies is drawn from a probability distribution $\{\Lambda_\ell\}$, so that ℓ replicas are sent with probability Λ_ℓ . Following a common notation inspired by codes on graphs [10], [39], [40], we will also compactly denote the distribution using a polynomial formulation as

$$\Lambda(x) = \sum_{\ell} \Lambda_{\ell} x^{\ell}.$$

Each copy contains a pointer to the positions of its twins within the frame, so that, upon retrieving one instance of a packet, the receiver is able to locate other replications.⁴ At the sink side, the decoding process initiates once the whole frame has been buffered. Specifically, the receiver

³Each node can then be thought of as a one-packet sized buffer, with preemption by fresher updated allowed only in waiting.

⁴This could be achieved, for instance, by explicitly adding the slot indexes using dedicated header fields.. A more efficient alternative which avoids overhead consists in using the payload as seed for a random number generator, used both at the sender and receiver side to place and locate replicas.

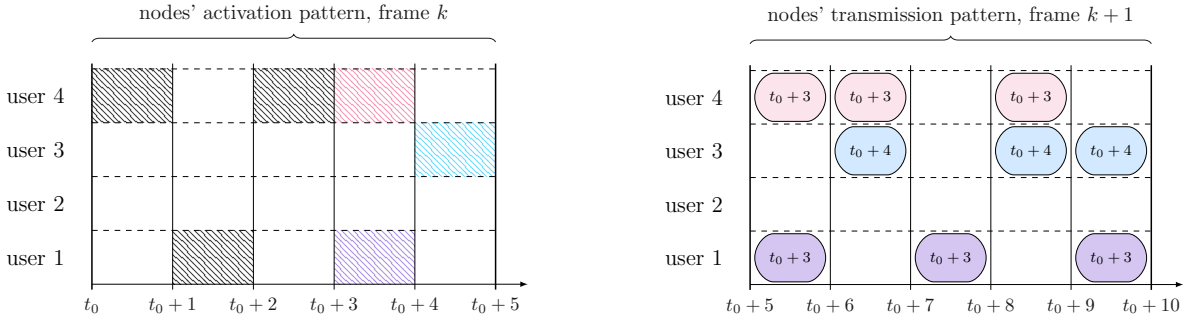


Fig. 2. Example of operation for IRSA with $n = 4$, $m = 5$. On the left handside, the activation pattern of users during a generic frame k is reported, assuming it starts at time t_0 . Filled rectangles indicate slots in which a node became active: note that only the last update (colour fill) will be sent. The right handside shows how nodes access the channel over the subsequent frame $k + 1$. Each node that became active transmits three replicas of its update, i.e. $\Lambda(x) = x^3$. Every replica contains the time at which the update was created: for instance, user 1 transmits the (freshest) packet that it generated at time $t_0 + 3$. At the receiver side, processing of frame $k + 1$ starts with the decoding of the interference-free second replica of user 1. Then, the contribution of its twins is removed (SIC), rendering the third copy of the packet of user 3 decodable. Finally, the update of user 4 can also be retrieved.

starts by looking for slots containing a single packet. For any such time unit, the corresponding update is decoded, and the interference contribution of all its replicas is removed from the frame, possibly leading to more singleton – and decodable – slots. The SIC procedure is iterated until all users have been retrieved or no more slots with a single packet can be found. An example of these working procedures is reported and discussed in Fig. 2.

For the considered traffic generation profile, the number of users that transmit over a frame is readily characterised by a binomial r.v. of parameters $(n, 1 - (1 - \rho)^m)$. Accordingly, the channel load G , defined as the average number of devices accessing the channel per slot, follows as

$$G = \frac{n [1 - (1 - \rho)^m]}{m}.$$

On the other hand, determining whether a message is correctly retrieved would require tracking the evolution of the SIC process over the finite-length time horizon of a frame. Due to the complexity of such task, an exact formulation of the packet loss rate P_l for IRSA, i.e. of the probability for a sent packet not to be decoded at the sink, has proven elusive to date. To characterise the performance of the scheme we then resort to an analytical approximation of P_l , combining two recent results. The first, introduced in [39], captures the behaviour of the protocol in the *error floor* region, i.e. for lightly loaded channels, whereas the second [40] offers

a performance estimate in the *waterfall region*, i.e. for medium to high levels of congestion, adapting the finite length scaling analysis of low-density parity check codes originally proposed in [41]. In both cases, a closed form approximation of the packet loss rate is offered as a function of the channel load, which we denote as $P_{l,ef}(G)$ (error-floor region) and $P_{l,wf}(G)$ (waterfall region), respectively. Due to space constraints, we do not report here the lengthy yet well known formulations, and refer the interested readers to the original papers for more details. More interestingly, instead, we observe that, despite being defined for any G , $P_{l,ef}(G)$ and $P_{l,wf}(G)$ capture effects that crucially impact performance in one of the two load regions, having little effect on the other one. This behaviour is well exemplified by the dashed curves in Fig. 3, which depict the trend of the two expressions for $\Lambda(x) = x^3$ and a frame of duration $m = 500$ slots. Leaning on this observation we then approximate the packet loss rate of IRSA for a generic channel load as

$$P_l(G) \simeq P_{l,ef}(G) + P_{l,wf}(G). \quad (5)$$

The good tightness of the approach is shown for different frame durations in Fig. 3, where (5) is shown by solid lines, while markers indicate the results of dedicated Montecarlo simulations.

Furthermore, the plot showcases a well-known effect, pinpointing how operating IRSA over longer frames triggers better performance, lowering the error floor and shifting the threshold for entering the waterfall region to higher channel loads [39], [40]. Finally, (5) allows to mathematically gauge the aggregate throughput, which can simply be expressed as

$$S = G(1 - P_l). \quad (6)$$

Let us now focus on the AoI evolution experienced by a node when IRSA is employed (see, e.g., Fig. 1b). Due to the operation mode of the protocol, $\delta^{(i)}(t)$ grows linearly over a frame, and is reset at the end of it with probability

$$\xi := [1 - (1 - \rho)^m] \cdot (1 - P_l) = \frac{mS}{n} \quad (7)$$

i.e. if an update was transmitted and successfully received at the sink. In such a case, the current AoI is refreshed to a value in the set $\{m + 1, \dots, 2m\}$.⁵ Indeed, at time of reception, m slots have elapsed for the transmission process, which add up to the initial offset due to the slots

⁵Note that we assume decoding to start only once the whole frame has been stored, and consider the time needed to perform SIC over a buffered m -slot period to be negligible compared to the duration of a frame, so that it does not affect the AoI value.

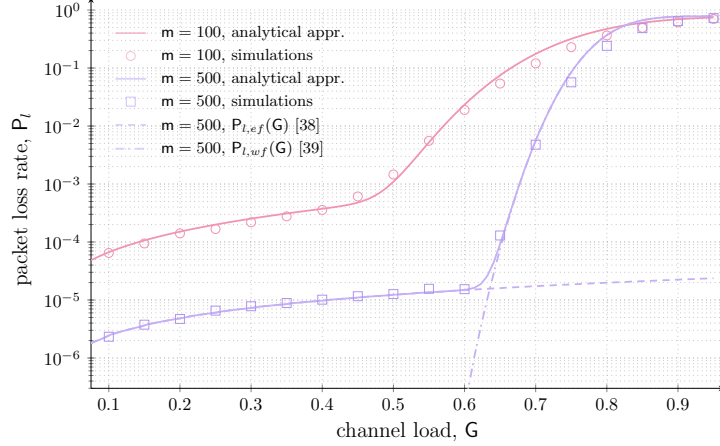


Fig. 3. IRSA packet loss rate vs. channel load, assuming $\Lambda(x) = x^3$. Solid lines report the analytical approximation in (5), while markers simulations.

between the generation of the packet and the opportunity for the node to access the channel at the start of the subsequent frame. Throughout our discussion, we describe the latter quantity via the discrete r.v. B , for which an example is given in Fig. 1b. Recalling the considered traffic generation model, B takes values in $\{1, \dots, m\}$ and has probability mass function (PMF)

$$p_B(b) = \frac{\rho(1-\rho)^{b-1}}{1-(1-\rho)^m}. \quad (8)$$

In the equation, the numerator captures the probability for the node to become active *for the last time* at the start of the $(m-b+1)$ -th slot of a frame, whereas the denominator imposes the normalisation condition that at least one packet has to be generated in the frame for the node to access the channel.

C. Notation

In conclusion, we introduce some useful notation often used in the remainder of the study. When analysing the behaviour of IRSA operated over frames of m slots, we shall decompose an integer value $n \in \mathbb{N}_0$ as

$$\begin{aligned} n &= \alpha_n + m\beta_n \\ \alpha_n &:= \text{mod}(n, m), \quad \beta_n := \lfloor n/m \rfloor \end{aligned} \quad (9)$$

In other words, we express a generic time slot index n as the sum of β_n frames and of α_n additional slots.

Moreover, given a discrete-time, discrete-valued Markov process X_n , $n \in \mathbb{N}$, we indicate its stationary distribution by $\{\pi_x\}$, $x \in \mathbb{N}$, when this exists. In this case, we refer as the *steady-state* version of the process to a r.v. X with PMF $\{\pi_x\}$.

III. ANALYSIS

We start our study by considering the current AoI, introduced in (1), when the system is operated following an IRSA access policy. Without risk of confusion we drop the node index i , and observe that the stochastic process $\delta(t)$ grows linearly within each frame, as its value can only be refreshed at the end of the m -slot period in case of successful reception of a time-stamped update. Accordingly, we can conveniently write

$$\delta(t) = \delta(m \cdot \lfloor t/m \rfloor) + \text{mod}(t, m) \quad (10)$$

where the first addend captures the age at the beginning of the current frame, while the second accounts for the additional offset from the start of the frame up to the observation time. Without loss of generality, we start tracking the process (i.e., set $t = 0$) right after the reception of the first update. Recalling the model introduced in Sec. II, the initial state of our system is thus in the set $\{m + 1, \dots, 2m\}$, and $\delta(t) \geq m + 1$, $\forall t$. Starting from these remarks, the evolution of the current age is completely specified by tracking the discrete time, discrete valued⁶ stochastic process

$$\Omega_k := \delta(km) - (m + 1), \quad k \in \mathbb{N}_0 \quad (11)$$

describing the offset of $\delta(t)$ at the beginning of the k -th frame with respect to its minimum possible value (see Fig. 1b).

Moreover, since each node operates independently over successive frames, i.e. the generation and one-shot transmission of a status update over m slots does not depend on previous outcomes, Ω_k is Markovian, and can be described by a chain with state space \mathbb{N}_0 . For such process, the one-step transition probabilities

$$q_{(i,j)} := \mathbb{P}\{\Omega_{k+1} = j \mid \Omega_k = i\}$$

can readily be computed noting that each frame sees a binary outcome, as either a successful update is delivered or the age continues to grow. Specifically:

⁶We remark that, while the process $\delta(t)$ takes values in \mathbb{R}^+ , the current AoI at the start of a frame can only be equal to an integer number of slots, by virtue of the slotted operation of the protocol described in Sec. II-B.

- the latter event takes place with probability $1 - \xi$, and in such condition the chain simply moves forward from state i to state $j = i + m$, tracking the linear increase of the AoI over the frame
- on the other hand, a status update for the node is retrieved with probability ξ , given in (7). In this case, the new AoI value at the start of frame $k + 1$ will be the sum of the m slots of frame k (needed to deliver the message with IRSA) and the additional slots elapsed between the generation of the update and the start of its transmission process, described by the r.v. B introduced in Sec. II-B. Accordingly, the Markov chain will transition from state i to state $j = B - 1$, $j \in \{0, \dots, m - 1\}$. For instance, if the successful message originated at the beginning of frame $k - 1$, i.e., $B = m$, the new age value at the start of frame $k + 1$ will be $2m$, so that the tracked process will be $m - 1$ slots above its minimum value. Similarly, if the device became active at the last slot of frame $k - 1$, we have $B = 1$, and the AoI will be reset to its minimum value $m + 1$, so that $\Omega_{k+1} = 0$.

Leaning on the PMF of the r.v. B given in (8), we can then write the transition probabilities for any state $i \in \mathbb{N}_0$ as

$$q_{(i,j)} = \begin{cases} \xi \cdot p_B(j + 1) & j \in \{0, \dots, m - 1\} \\ 1 - \xi & j = i + m \\ 0 & \text{otherwise} \end{cases} . \quad (12)$$

The formulation in (12) allows to compute the evolution of Ω_k at any point in time, given the initial condition of the system. In general, however, we are more interested in evaluating the long run behaviour of the current age, which we characterise via following result:

Proposition 1: The stochastic process Ω_k is ergodic, and has steady state distribution

$$\pi_\omega = \frac{mS}{n} \left(1 - \frac{mS}{n}\right)^{\beta_\omega} \cdot \frac{\rho(1 - \rho)^{\alpha_\omega}}{1 - (1 - \rho)^m}, \quad \omega \in \mathbb{N}_0 \quad (13)$$

where α_ω and β_ω are defined as per (9).

Proof: We start by observing that the Markov chain is irreducible, i.e. for any state-pair (i, j) , there exists $n > 0$ s.t. the n -step transition probability between the two states is strictly positive. If $j \in \{0 \dots, m - 1\}$ the statement holds already at one step from (12). Otherwise, leaning on (9), let us express $j = \alpha_j + m\beta_j$. Then, the transition from i to j can take place in $\beta_j + 1$ steps, moving to state $\alpha_j < m$ with a successful update, and then experiencing β_j

frames without managing to deliver a packet. The event has probability $q_{(i,\alpha_j)} \cdot (1 - \xi)^{\beta_j} > 0$, proving the irreducibility of the chain. Furthermore, observing that each state in $\{0, \dots, m - 1\}$ has period 1, the chain is also aperiodic, and admits thus an asymptotic probability distribution $\{\pi_\omega\}$. Writing the balance equations, we obtain from (12):

$$\begin{cases} \pi_\omega = \sum_{j=0}^{\infty} \pi_j \cdot \xi p_B(\omega + 1) \stackrel{(a)}{=} \xi p_B(\omega + 1) & \omega < m \\ \pi_\omega = \pi_{\omega-m} \cdot (1 - \xi) & \omega \geq m \end{cases} \quad (14a)$$

$$\pi_\omega = \pi_{\omega-m} \cdot (1 - \xi) \quad \omega \geq m \quad (14b)$$

where (a) stems from the normalisation condition $\sum_\omega \pi_\omega = 1$. For the expressions in (14b), decomposing the state index as in (9) and applying a simple recursion eventually leads to $\pi_\omega = \pi_{\alpha_\omega} \cdot (1 - \xi)^{\beta_\omega}$, where π_{α_ω} is given by the corresponding equation in (14a). Combining these results, we have, for any $\omega \in \mathbb{N}_0$

$$\pi_\omega = \xi(1 - \xi)^{\beta_\omega} \cdot p_B(\alpha_\omega + 1). \quad (15)$$

As the Markov chain admits a *proper* stationary distribution ($\pi_\omega > 0$), the process Ω_k is also positive recurrent, and thus ergodic. Plugging the expressions of ξ and $p_B(b)$ into (15) eventually leads to the statement formulation in (13). ■

Notably, the expression in (13) offers a compact closed-form statistical characterisation of the asymptotic behaviour of the instantaneous AoI of a node when the network is operated with an IRSA medium access, for any replica distribution $\{\Lambda_\ell\}$. Leaning on this general result, two quantities of particular interest for system design can be derived: average AoI and peak age violation probability, which we characterise in the remainder of the section.

A. IRSA average AoI

A first relevant performance benchmark to gauge the ability of a medium access scheme to keep up-to-date information at the receiver is the *average AoI*, formally defined in (2), for which we provide the following

Proposition 2: The average network AoI of IRSA, measured in slots and under the traffic model of Sec. II, is given by

$$\Delta_{\text{irsa}} = \frac{m}{2} + \frac{n}{S} + \left(\frac{1}{\rho} - \frac{m(1 - \rho)^m}{1 - (1 - \rho)^m} \right). \quad (16)$$

Proof: Let us focus on a generic node i , for which we aim at computing the time average introduced in (3), and express the observation interval as $t = km + \text{mod}(t, m)$, i.e. k entire frames plus a portion of the $(k + 1)$ -th m -slot period. Asymptotically, the contribution of the second addend becomes negligible, so that

$$\begin{aligned}\Delta^{(i)} &= \lim_{k \rightarrow \infty} \frac{1}{km} \int_0^{km} \delta^{(i)}(\tau) d\tau \\ &= \lim_{k \rightarrow \infty} \frac{1}{km} \sum_{\ell=0}^{k-1} \int_{\ell m}^{(\ell+1)m} (m + 1 + \Omega_\ell + \tau) d\tau\end{aligned}$$

expressing the integral as the sum of its components over the k observed periods, and decomposing the age over a frame as the sum of its value at the start of the m -slot interval and of a linear offset as specified by (10), (11). After simple manipulations:

$$\Delta^{(i)} = 1 + \frac{3m}{2} + \lim_{k \rightarrow \infty} \frac{1}{k} \sum_{\ell=0}^{k-1} \Omega_\ell \stackrel{(a)}{=} 1 + \frac{3m}{2} + \sum_{\omega=0}^{\infty} \omega \pi_\omega \quad (17)$$

where (a) follows with probability 1 from the ergodicity of the Markov chain proven in Prop. 1 [42]. The average AoI for the node can then be computed by evaluating the expected value of the stationary distribution of the stochastic process Ω_k . Using the formulation for π_ω in (15) and expressing once more $\omega \in \mathbb{N}_0$ as $\omega = \alpha_\omega + m\beta_\omega$:

$$\begin{aligned}\sum_{\omega=0}^{\infty} \omega \pi_\omega &= \sum_{\beta_\omega=0}^{\infty} \sum_{\alpha_\omega=0}^{m-1} (\alpha_\omega + m\beta_\omega) \xi(1 - \xi)^{\beta_\omega} p_B(\alpha_\omega + 1) \\ &= m \sum_{\beta_\omega=0}^{\infty} \beta_\omega \xi(1 - \xi)^{\beta_\omega} + \sum_{\alpha_\omega=0}^{m-1} \alpha_\omega p_B(\alpha_\omega + 1).\end{aligned}$$

If we now observe that

$$\begin{aligned}m \sum_{\beta_\omega=0}^{\infty} \beta_\omega \xi(1 - \xi)^{\beta_\omega} &= \frac{m(1 - \xi)}{\xi} = \frac{n}{S} - m \\ \sum_{\alpha_\omega=0}^{m-1} \alpha_\omega p_B(\alpha_\omega + 1) &= \frac{1}{\rho} - 1 - \frac{m(1 - \rho)^m}{1 - (1 - \rho)^m}\end{aligned}$$

and plug these values into (17), the right hand-side of the proposition statement follows. Recalling that all nodes in the system operate independently, we have

$$\Delta_{\text{irsa}} = \frac{1}{n} \sum_{i=1}^n \Delta^{(i)} = \Delta^{(i)}$$

concluding the proof. ■

Incidentally, we note that the statement of Prop. 2 offers an alternative and more general derivation of the result originally presented in [37] via area calculation arguments, proving in addition the existence of the limit in (3).

B. IRSA peak age violation probability

Aiming at an educated system design, the behaviour of an access scheme in terms of average AoI shall be complemented by a characterisation of the distribution tail. This is especially relevant, e.g., for critical applications and control of dynamic systems, where relying on exceedingly stale information may have dire consequences. A relevant metric to tackle this aspect is the peak age violation probability, originally introduced in [38], and receiving further attention in recent years, see, e.g. [43], [44], [45].

In this perspective, we focus on the long term behaviour of the system, and introduce the following

Definition 1: The IRSA peak age violation probability, $\zeta(\theta)$, is the probability that the steady-state version of the current AoI for a user exceeds a threshold value θ . Recalling the linear growth of $\delta^{(i)}(t)$ over an m -slot period, this occurs if the value of the steady-state process capturing the age at the start of the frame is higher than $\theta - m$. From (11) we then formally have

$$\zeta(\theta) := \mathbb{P}\{\Omega > \theta - 2m - 1\}$$

where the r.v. Ω with PMF corresponding to the asymptotic distribution of the process Ω_k , i.e., $p_{\Omega}(\omega) = \pi_{\omega}$, is introduced in accordance to Sec. II-C.

We remark that, thanks to the ergodicity of the Markov process, ζ also corresponds to the fraction of the frames in which the receiver experiences an AoI above a target value, offering thus an intuitive and useful design tool. Leaning on this definition, we prove the following closed-form result

Proposition 3: The peak age violation probability $\zeta(\theta)$ for IRSA under the traffic model of Sec. II is given by

$$\zeta(\theta) = \begin{cases} \frac{mS}{n} \left(1 - \frac{mS}{n}\right)^{\beta_{\theta-2m}} \cdot \frac{(1-\rho)^{1+\alpha_{\theta-2m}} - (1-\rho)^m}{1 - (1-\rho)^m} + \left(1 - \frac{mS}{n}\right)^{1+\beta_{\theta-2m}} & \theta > 2m \\ 1 & \text{otherwise} \end{cases} \quad (18)$$

where the ancillary quantities $\alpha_{\theta-2m}$ and $\beta_{\theta-2m}$ are defined as per (9).

Proof: Recalling that the current AoI for a device is never lower than $m + 1$ slots, and that the value grows linearly over a frame, we readily have $\zeta(\theta) = 1$ for $\theta < 2m + 1$. For larger values, let us introduce for compactness the auxiliary variable $\theta' := \theta - 2m$, and express it as $\theta' = \alpha_{\theta'} + m\beta_{\theta'}$ following the notation of (9). Accordingly, we can write

$$\zeta(\theta) = \sum_{\omega=\theta'}^{\infty} \pi_{\omega} = \sum_{\ell=1+\alpha_{\theta'}}^{m-1} \pi_{\ell+m\beta_{\theta'}} + \sum_{j=1+\beta_{\theta'}}^{\infty} \sum_{\ell=0}^{m-1} \pi_{\ell+mj}$$

where the second equality stems from decomposing $\omega = \alpha_{\omega} + m\beta_{\omega}$. With this approach, indeed, the first summation accounts for the case of having the r.v. Ω composed by the same number of frames as θ' yet by more additional slots, whereas the second summation for the remaining case $\beta_{\omega} > \beta_{\theta'}$. Plugging in the formulations of (15) and (8),

$$\zeta(\theta) = \xi(1 - \xi)^{\beta_{\theta'}} \cdot \sum_{\ell=1+\alpha_{\theta'}}^{m-1} \frac{\rho(1 - \rho)^{\ell}}{1 - (1 - \rho)^m} + (1 - \xi)^{\beta_{\theta'}+1}$$

observing that $\sum_{\ell=1}^{m-1} p_B(\ell) = 1$ and recalling that $\sum_{j=1+\beta_{\theta'}}^{\infty} (1 - \xi)^j = (1 - \xi)^{\theta'}/\xi$. Solving the remaining summation and substituting the value of ξ derived in (7) leads to (18). ■

Before moving to an in-depth discussion of the performance achieved by IRSA, two observations are in order. First, it is relevant to stress that the presented framework offers exact closed-form expressions of both average AoI and peak age violation probability. On the other hand, these quantities are a function of S , for which, as discussed, no compact characterisation is known to date. In the remainder of our study we will then evaluate the performance of the protocol resorting to the tight analytical approximation in (5), yet note how the results can be applied to any other (approximated or – if available – exact) IRSA throughput formulation.

Secondly, the analysis that we propose goes beyond the specific protocol operation of IRSA, and can capture the performance of a broader class of schemes. Indeed, equations (16) and (18) hold, under the traffic model of Sec. II, for any framed slotted ALOHA approach as long as the proper throughput characterisation is employed. From this standpoint, for instance, the framework also applies to the coded slotted ALOHA family [10], as well as to T-fold SA [46].

C. Reference Benchmark: slotted ALOHA

To better gauge the behaviour of IRSA, we complement our analysis by deriving the AoI statistics for a simpler SA policy. In this case, the communication process is not bound to a framed structure, and an update is transmitted as soon as it is generated. Focusing on a generic

time instant t within the k -th slot, i.e. $t = k + \text{mod}(t, k)$, the current age for a node can thus be expressed as

$$\delta_{\text{sa}}(t) = \delta_{\text{sa}}(k) + \text{mod}(t, k).$$

Therefore, the AoI evolution can be completely specified by characterising the discrete-time, discrete-valued stochastic process

$$\Psi_k := \delta_{\text{sa}}(k) - 1, \quad k \in \mathbb{N}_0 \quad (19)$$

which tracks the offset of the AoI at the start of slot k with respect to the minimum possible value 1 (see Fig. 1a). Also in this case, the process is Markovian, and, recalling (4), from any state j the chain may either transition to state 0 with probability ξ_{sa} , or to state $j + 1$ with probability $1 - \xi_{\text{sa}}$. Following a reasoning similar to the one of Prop. 1, the process can readily be shown to be ergodic, and with stationary distribution $\pi_\psi = \xi_{\text{sa}}(1 - \xi_{\text{sa}})^k$, $k \in \mathbb{N}_0$.

As done for IRSA, we can furthermore study the tail of the age distribution by introducing

Definition 2: The SA peak age violation probability, $\zeta_{\text{sa}}(\theta)$, is the probability that the steady-state version of the current AoI for a user exceeds a threshold θ , or, equivalently, the fraction of slots that experience an age above θ asymptotically. From (19), we have

$$\zeta_{\text{sa}}(\theta) = \mathbb{P}\{\Psi > \theta - 2\}$$

where Ψ is again introduced for ease of notation as a r.v. having PMF $p_\Psi(\psi) = \pi_\psi$.

Accordingly, we can summarise the behaviour of the protocol with a simple result:

Proposition 4: For a SA system, under the traffic model of Sec. II, the average network AoI – expressed in slots – and the peak age violation probability are given by

$$\Delta_{\text{sa}} = \frac{1}{2} + \frac{n}{S_{\text{sa}}}, \quad \zeta_{\text{sa}}(\theta) = \begin{cases} (1 - \xi_{\text{sa}})^{\theta-1} & \theta > 1 \\ 1 & \text{otherwise} \end{cases} \quad (20)$$

Proof: The average age can be obtained via simple calculations applying the same approach presented in Prop. 2, whereas the peak age violation immediately follows as the complementary CDF of the geometric r.v. Ψ . ■

The presented result for the average AoI is in agreement with the formulations originally presented in [32], [33], although obtained in our case from the statistics of the Markov chain. Moreover, to the best of our knowledge, this is the first characterisation of the peak age violation probability in a SA setup.

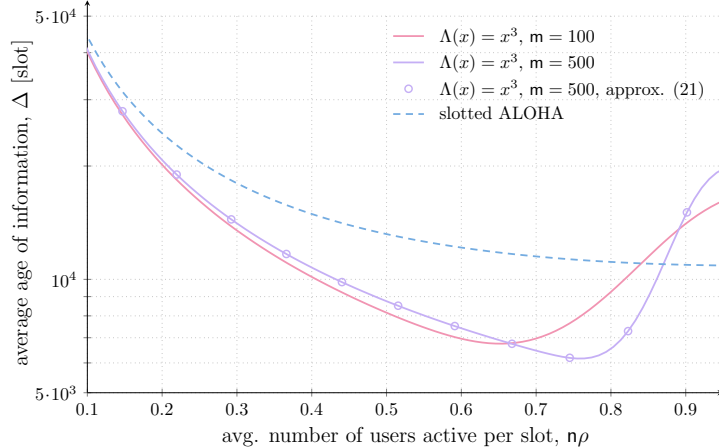


Fig. 4. Average network AoI Δ vs. average number of active users per slot $n\rho$ for SA (dashed line), and IRSA (solid lines). All results were obtained for $n = 4000$ users and, for IRSA, $\Lambda(x) = x^3$.

IV. RESULTS AND DISCUSSION

A. Average age of information

To draw insights on the behaviour of the considered protocols, we start by studying the average network AoI. Unless otherwise stated, we consider a system with $n = 4000$ terminals, and assume a distribution $\Lambda(x) = x^3$ for IRSA operations (i.e., a node accessing the channel sends three copies of its packet over the frame). Focusing on this configuration, Fig. 4 reports the trends of Δ_{irsa} (solid lines) and Δ_{sa} (dashed line) as a function of the average number of users per slot that generate an update ($n\rho$).

All access policies exhibit a common behaviour as nodes' activity increases, characterised by a point of minimum for the average AoI experienced at moderate-to-high channel load. Indeed, while a lightly loaded medium grants high chance of success for a transmitted update, the behaviour for low values of $n\rho$ is driven by the scarce activity of terminals, resulting in long inter-update generation times (low ρ) that penalise Δ . Conversely, too frequent reporting from nodes ($n\rho \sim 1$) lead to channel congestion, hindering decoding of information at the receiver due to collisions.

More interestingly, Fig. 4 highlights how IRSA consistently outperforms SA in terms of average AoI for most values of $n\rho$, and triggers stark improvements exactly in the moderate load conditions under which many practical systems are operated. The trend is buttressed by Tab. I, which summarises the ratio $\Delta_{\text{irsa}}/\Delta_{\text{sa}}$ for different user populations and different channel

TABLE I

$\Delta_{\text{irsa}}/\Delta_{\text{sa}}$ FOR DIFFERENT POPULATIONS (n) AND AVERAGE NUMBER OF USERS BECOMING ACTIVE PER SLOT ($n\rho$). FOR IRSA, $m = 500$ AND $\Lambda(x) = x^3$.

$n\rho$ [usr/slot]	$n = 2000$	$n = 4000$	$n = 6000$
0.2	0.8801	0.8494	0.8392
0.4	0.7708	0.7206	0.7038
0.8	0.5955	0.5879	0.6096

occupancies. Such a result is non-trivial, as it clarifies how the benefits in terms of throughput efficiency offered by repetitions and SIC do outweigh the additional latency cost induced by framed channel access. A first relevant design hint is thus offered, suggesting the use of modern random access solutions as a means to reduce AoI in grant-free based mMTC applications.

Moreover, Fig. 4 prompts the natural question on what are the best working conditions (e.g., in terms of $n\rho$) and how shall systems parameters be tuned in order to optimise AoI performance. To tackle this design facet, let us first focus on SA. In this case, an inspection of (20) readily reveals how – for a given terminal population n – the minimum AoI Δ_{sa}^* is achieved when the aggregate throughput S is maximised. This happens for $\rho = 1/n$, leading to

$$\Delta_{\text{sa}}^* = \frac{1}{2} + n \left(1 - \frac{1}{n}\right)^{1-n} \simeq \frac{1}{2} + ne$$

where the approximation quickly becomes tight for large enough, and practical, values of n . As to IRSA, instead, changes in the activation probability ρ affect not only the throughput, but also the additional term accounting for the latency between update generation and transmission (i.e., the third addend in (16)), prompting a more convoluted dependency of Δ_{irsa} on the channel contention factor $n\rho$. To further delve into this aspect, let us focus on the typical configurations of mMTC applications, characterised by devices that become active in a sporadic fashion (i.e. $\rho \ll 1$). Under this assumption – which also holds in our setup – we can apply the Taylor series expansion $(1 - \rho)^m \simeq 1 - m\rho + m(m-1)\rho^2/2$ to (16), to obtain, after few simple manipulations, the simpler formulation

$$\Delta_{\text{irsa}} \simeq \frac{1}{2} + \frac{n}{S} + m \quad (21)$$

reported by circle markers in Fig. 4 for the case $m = 500$. The approximation in (21) allows to draw some interesting remarks. First, it clarifies how, when the frame size is fixed, the

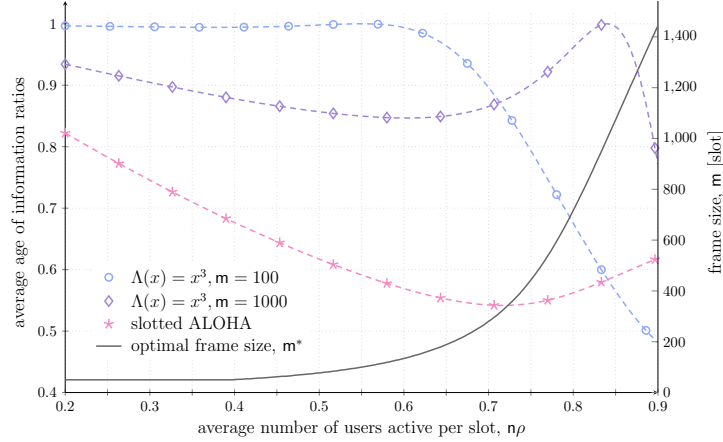


Fig. 5. Dashed lines, referring to the left y -axis, report the ratio of the average AoI obtained by optimising IRSA frame size to the average AoI achieved by other schemes. Specifically, circle markers indicate the ratio for IRSA operated over $m = 100$ slots, diamond markers for IRSA with $m = 1000$ slots, and star markers for SA. The solid line, referring to the right y -axis, reports the optimal frame size m^* for IRSA. All results obtained for $n = 4000$ users and, for IRSA, $\Lambda(x) = x^3$.

average AoI is minimised also for IRSA by operating the system around its maximum throughput conditions.⁷ Secondly, the result offers a handy parallel with SA – for which $\Delta_{sa} = 1/2 + n/S_{sa}$ (Prop. 4) –, revealing an additional penalty of m slots experienced by IRSA. This term stems from the very operation mode of the protocol, which entails a whole frame duration to transmit and decode a message ($m/2$ average AoI component already present in (16)), and forces a newly generated update to await the start of the next frame to be sent ($1/2 + m/2$ contribution to Δ_{irsa} when $\rho \ll 1$). From this standpoint, (21) pinpoints a fundamental tradeoff for the behaviour of IRSA, stressing how throughput is not the only force driving information freshness. Indeed, while operating over longer frames leads to lower packet loss rates - and thus higher S – for any channel load of practical relevance (see Fig. 3), it also increases the penalty term m , possibly worsening the average AoI.

The critical role played by m is explored in more depth in Fig. 5. Specifically, the solid line, whose values are referred to the right y -axis in the plot, shows the optimal frame length m^* at which IRSA shall be operated for different channel occupancies $n\rho$ in order to minimise

⁷This result may, for instance, be useful in the presence of a feedback channel. In this case, the sink could estimate the experience channel load, and distribute an access probability to the devices so as to improve the AoI performance.

the average AoI.⁸ The trend clearly highlights how small values of m shall be preferred in lightly loaded channels, while longer frames become beneficial when more devices concurrently access the medium. With low node activity, in fact, IRSA operates in the error-floor region ($P_l \ll 1$), where an increase in frame size does not trigger significant changes in the achievable throughput, rendering m the driving factor for Δ_{irsa} . Conversely, at higher load, longer frames allow retrieval of a substantially larger number of updates, and the throughput gain more than compensates the additional latency penalty. In this perspective, it is also interesting to gauge how much benefit a tailored frame duration may bring. The question is tackled once more by Fig. 5, where the dashed lines, referred to the left y -axis, specify the ratio of the average AoI obtained by optimising m to the performance achieved otherwise. Specifically, circle markers indicate such ratio when IRSA is operated over a frame of length $m = 100$ slots, irrespective of the channel load, while diamond markers refer to the case $m = 1000$. Finally, the star markers show the ratio of the optimised IRSA average AoI to the performance of SA (i.e., to Δ_{sa}). The importance of properly selecting m clearly emerges, becoming especially critical at intermediate channel loads. Indeed, while the loss undergone for employing long frames in lightly loaded channels is rather contained ($\sim 10\%$), operating the system with suboptimal values of m can lead to stark performance losses when devices become active more frequently. It is also relevant to observe that – going beyond the specific outcomes that were illustrated in Fig. 4 – a properly operated version of IRSA can outperform SA in terms of average AoI even for larger values of channel load (e.g., $n\rho \simeq 0.9$).

All results presented so far were obtained by assuming that each device transmits three copies of its packet over a frame, i.e. relying on $\Lambda_1(x) = x^3$. To complement our discussion, we further study the impact of using different degree distributions. Specifically, we focus on the average AoI achieved with a simple regular distribution of higher degree, $\Lambda_2(x) = x^4$, and with the irregular distribution $\Lambda_3(x) = 0.86x^3 + 0.14x^8$, originally derived in [39] via an optimisation that accounts for performance both in the error-floor and waterfall regions. The behaviour of Δ_{irsa} using the different PMFs is reported in Fig. 6 when changing the frame size m and for two distinct values of $n\rho$. The trends can be properly interpreted recalling the performance induced by the IRSA distribution on packet loss rate and throughput, shown for convenience in

⁸The reported values have been derived by simple numerical minimisation of (16), analytically obtaining the system throughput via the approximation discussed in (5) and (6).

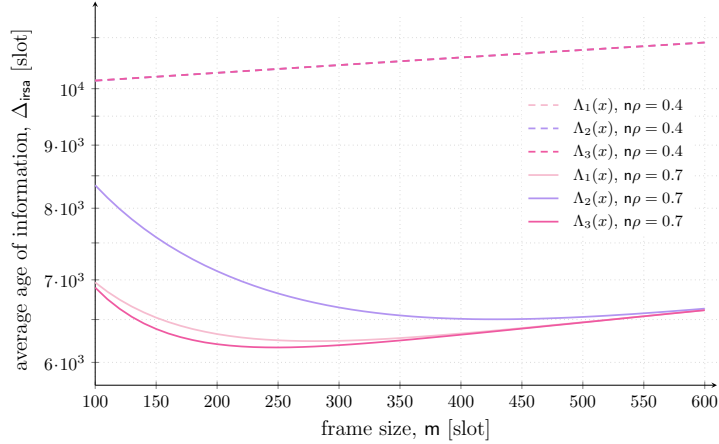


Fig. 6. Average network AoI Δ vs. frame size m for different IRSA distributions and different value of $n\rho$. $n = 4000$ users.

Fig. 7 against $n\rho$ for two relevant frame sizes. Let us first focus on a lightly loaded channel, considering the case $n\rho = 0.4$, i.e. dashed lines in Fig. 6. In such conditions, all PMFs deliver very similar performance. Indeed, IRSA is operating in the error-floor region even for short frame sizes ($m = 100$), so that the beneficial effects on the packet loss rate brought by having users sending more replicas (Fig. 7a) do not translate into substantial throughput – and AoI – improvements (Fig. 7b). Instead, the role played by more refined transmission probability distributions kicks in in congested channels, prompting significant differences on the achievable $\Delta_{\text{irsā}}$ (solid curves in Fig. 6, $n\rho = 0.7$). If we compare, for instance, the behaviour of $\Lambda_2(x)$ and $\Lambda_3(x)$ for $m = 100$ in Fig. 7, it is apparent how the former distribution is already operating beyond its throughput peak, whereas the optimised replica transmission probabilities of the latter enable relevant throughput gains. The effect becomes less pronounced for longer frame sizes, as all the considered distributions tend to perform similarly, leading to the convergence of the average AoI curves in Fig. 6. From this standpoint, the plot prompts two further relevant remarks. First, the frame size granting the best performance is tightly related to the employed distribution – e.g., for $n\rho = 0.7$, $m \simeq 250$ shall be chosen when using $\Lambda_3(x)$, whereas $m \simeq 420$ is optimal for $\Lambda_2(x)$. Secondly, the notable gains that emerge were obtained by analysing some simple and well-known distributions, while a dedicated optimisation of the distribution $\Lambda(x)$ focusing on AoI-based metrics may further improve performance.

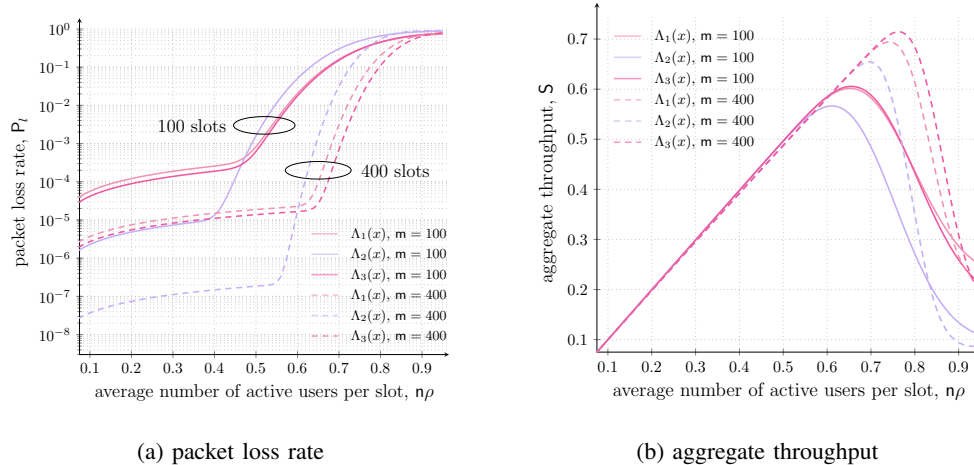


Fig. 7. Packet loss rate (a) and aggregate throughput (b) vs. average number of active users per slot ($m\rho$) for different IRSA distributions. Solid lines show the behaviour when operating the system over frames of 100 slots, whereas solid lines consider $m = 400$. In all cases, $n = 4000$.

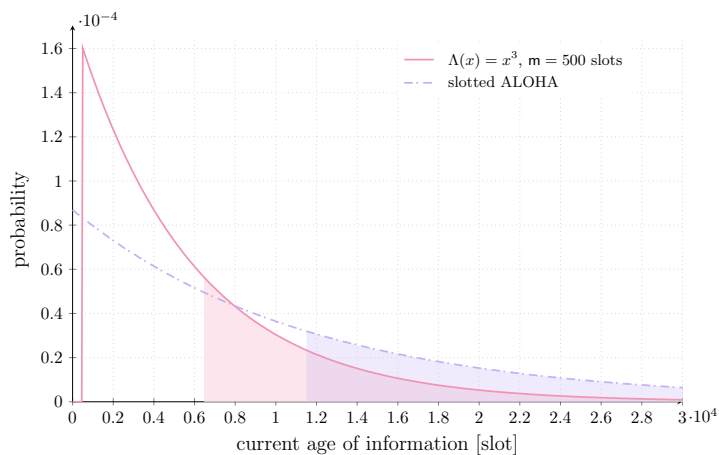


Fig. 8. Stationary PMF of the current age at the start of a frame for IRSA (solid line) and at the start of a slot for SA (dashed line). For IRSA, $\Lambda(x) = x^3$ was considered. In all cases, $n = 4000$, $n\rho = 0.7$.

B. Peak age violation probability

Additional system design hints can be derived by looking at tail of the AoI process of the considered medium access schemes. To this aim, Fig. 8 reports for $n\rho = 0.7$ the stationary distributions of the current age for a node derived in Prop. 3 and 4. Specifically, the solid curve indicates the age PMF at the start of a frame for IRSA (i.e. the distribution of the r.v. $m + 1 + \Omega$), while the dashed one the age PMF at the start of a slot for SA (i.e. the distribution of the r.v. $1 + \Psi$). As expected, SA has a non-null probability to experience very low values, whereas the

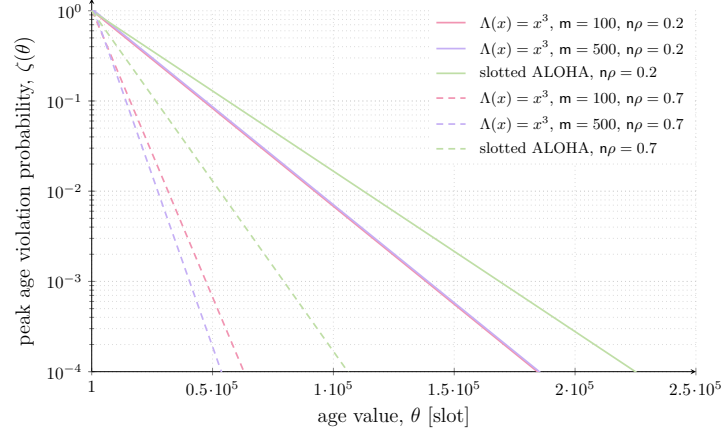


Fig. 9. Peak age violation probability for slotted ALOHA and IRSA. Solid lines report the trends for $n\rho = 0.2$, whereas dashed ones for $n\rho = 0.7$. For IRSA, $\Lambda(x)^3$ and, in all cases, $n = 4000$.

framed operations of IRSA bound age to a minimum of $m + 1$ slots. Conversely, the better packet delivery probability of the modern random access scheme leads to a sharper initial spike of the PMF, yielding an overall lower value of average AoI.

More interestingly, the filled areas in the plot highlight values of age that exceed the average for the schemes, revealing in both cases a significant – yet differently shaped – tail, and stressing the importance of the peak age violation probability in properly gauging the performance of the protocols. The metric behaviour is shown in Fig. 9 considering both a lightly loaded ($n\rho = 0.2$, solid lines) and a more congested ($n\rho = 0.7$, dashed lines) channel. In all conditions, IRSA outperforms SA, significantly lowering the probability of exceeding a threshold value of tolerable age of information. Moreover, the plot pinpoints that longer frames are to be preferred at intermediate to high channel loads from a peak age violation probability standpoint as well. On the other hand, only small improvements are attained in lighter traffic conditions by operating the scheme over shorter frames.

These trends are further explored in Fig. 10, depicting as a function of $n\rho$ the AoI threshold θ^* for which a target peak age violation probability ζ^* is reached, i.e. such that $\zeta(\theta^*) = \zeta^*$. In other words, dashed lines report the AoI which is exceeded in less than 10% (dashed lines) and 0.1% (solid lines) of the frames for IRSA (or slots, for SA). In this perspective, the plot can be seen as a practical tool for system design, allowing an educated choice of the operating parameters based on the desired – and achievable – performance, for which the presented framework offers effective closed-form expressions. The result confirms how important gains can be achieved

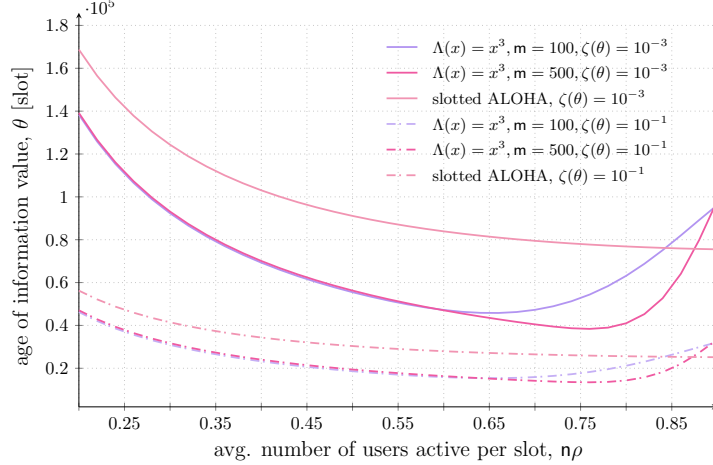


Fig. 10. Age of information value for which a target peak violation probability is reached, reported against $n\rho$. Dashed lines refer to a target $\zeta = 10^{-1}$, whereas solid lines to $\zeta = 10^{-3}$. $n = 4000$, and $n\rho = 0.7$.

by resorting to the modern random access solution, with θ almost halved compared to SA for channel occupancies or practical relevance (e.g., $n\rho \simeq 0.7$). Furthermore, in spite of the slightly more complex formulation in (18), the fundamental trade-offs discussed for the average AoI are confirmed also when looking at the age distribution tail, showing how good performance can be achieved in high throughput conditions, and stressing the important role played by the selected frame duration.

V. CONCLUSIONS

This paper offered the first analytical characterisation of a class of modern random access scheme from an information freshness standpoint. Specifically, focusing on the irregular repetition slotted ALOHA (IRSA) protocol, the evolution of the current AoI for a status update source has been tracked by means of a Markov chain, which was proven to be ergodic. Leaning on a closed-form expression for the stationary distribution of such process, simple exact expressions for the average AoI and for the peak age violation probability were discussed. The presented analysis revealed how IRSA can significantly outperform slotted ALOHA with respect to both metrics, and pinpointed some fundamental trade-offs that drive the behaviour of the protocol, capturing the impact of frame length and replica number distribution. The compact formulations introduced in the article offer a simple yet effective tool for proper system design.

REFERENCES

- [1] W. Saad, M. Bennis, and M. Chen, "A vision of 6G wireless systems: Applications, trends, technologies, and open research problems," *IEEE Network*, vol. 34, no. 3, pp. 134–142, 2020.
- [2] G. Flagship, "Critical and Massive Machine Type Communication Towards 6G," 2020. [Online]. Available: <http://arxiv.org/abs/2004.14146>
- [3] I. LeyvaMayorga, C. Stefanovic, P. Popovski, V. Pla, and J. MartinezBauset, "Random access for machinetype communications," *Wiley 5G Ref*, 2019.
- [4] N. Abramson, "The ALOHA System - Another Alternative for Computer Communications," in *Proc. 1970 Fall Joint Computer Conference*. AFIPS Press, 1970.
- [5] LoRa Alliance Technical Committee, "LoRaWAN 1.1 Specification."
- [6] Sigfox, "SIGFOX: The Global Communications Service Provider for the Internet of Things," www.sigfox.com.
- [7] Y. . E. Wang, X. Lin, A. Adhikary, A. Grovlen, Y. Sui, Y. Blankenship, J. Bergman, and H. S. Razaghi, "A primer on 3GPP narrowband internet of things," *IEEE Communications Magazine*, vol. 55, no. 3, pp. 117–123, 2017.
- [8] 3GPP, "RP-193143: Rel17 study item on NB-Io/eMTC support for non-terrestrial networks," 2020.
- [9] M. Berioli, G. Cocco, G. Liva, and A. Munari, *Modern random access protocols*. NOW Publisher, 2016.
- [10] E. Paolini, G. Liva, and M. Chiani, "Coded Slotted ALOHA: A Graph-Based Method for Uncoordinated Multiple Access," *IEEE Trans. Inf. Theory*, vol. 61, no. 12, pp. 6815–6832, 2015.
- [11] F. Clazzer, C. Kissling, and M. Marchese, "Enhancing Contention Resolution ALOHA using Combining Techniques," *IEEE Trans. Commun.*, vol. 66, no. 6, pp. 2576–2587, 2018.
- [12] Y. Polyanskiy, "A Perspective on Massive Random-Access," in *Proc. IEEE ISIT*, 2017.
- [13] C. Stefanovic and P. Popovski, "ALOHA Random Access that Operates as a Rateless Code," *IEEE Commun. Mag.*, vol. 61, no. 11, pp. 4653–4662, 2013.
- [14] V. Amalladinne, J.-F. Chamberland, and K. Narayanan, "An Enhanced Decoding Algorithm for Coded Compressed Sensing," 2019. [Online]. Available: <http://arxiv.org/abs/1910.0974>
- [15] A. Fengler, P. Jung, and G. Caire, "SPARCs and AMP for Unsourced Random Access," in *Proc. IEEE ISIT*, 2019.
- [16] S. S. Kowshik, K. Andreev, A. Frolov, and Y. Polyanskiy, "Energy efficient coded random access for the wireless uplink," *IEEE Transactions on Communications*, 2020.
- [17] G. Liva, "Graph-Based Analysis and Optimization of Contention Resolution Diversity Slotted ALOHA," *IEEE Trans. Commun.*, vol. 59, no. 2, pp. 477–487, 2011.
- [18] ETSI, "EN 301 545-2: Digital Video Broadcasting (DVB); Second Generation DVB Interactive Satellite System (DVB-RCS2); Part 2: Lower Layers for Satellite standard," Tech. Rep., 2014.
- [19] Y. Sun, Y. Polyanskiy, and E. Uysal, "Sampling of the Wiener Process for Remote Estimation over a Channel with Random Delay," *IEEE Trans. Inf. Theory*, 2020.
- [20] A. Maatouk, S. Kriouile, M. Assaad, and A. Ephremides, "The Age of Incorrect Information: a new Performance Metric for Status Updates," 2019. [Online]. Available: <http://arxiv.org/abs/1907.06604v1>
- [21] T. Soleymani, J. Baras, and S. Hirche, "Value of Information in Feedback Control," *IEEE Trans. Autom. Control*, 2020.
- [22] S. Kaul, M. Gruteser, V. Rai, and J. Kenney, "Minimizing age of information in vehicular networks," in *Proc. IEEE SECON*, June 2011.
- [23] S. Kaul, R. Yates, and M. Gruteser, "On piggybacking in vehicular networks," in *Proc. IEEE GLOBECOM*, Dec 2011.
- [24] Y. Sun, I. Kadota, R. Talak, E. Modiano, and R. Srikant, *Age of Information: A New Metric for Information Freshness*. Morgan & Claypool, 2019.

- [25] R. D. Yates and S. K. Kaul, "The age of information: Real-time status updating by multiple sources," *IEEE Transactions on Information Theory*, vol. 65, no. 3, pp. 1807–1827, March 2019.
- [26] B. Zhou and W. Saad, "Minimum age of information in the internet of things with non-uniform status packet sizes," *IEEE Transactions on Wireless Communications*, vol. 19, no. 3, pp. 1933–1947, 2020.
- [27] A. Bedewy, Y. Sun, S. Kompella, and N. Shroff, "Age-optimal sampling and transmission scheduling in multi-source systems," in *Proc. ACM MOBIHOC*, 2019.
- [28] B. Zhou and W. Saad, "Joint status sampling and updating for minimizing age of information in the internet of things," *IEEE Transactions on Communications*, vol. 67, no. 11, pp. 7468–7482, 2019.
- [29] Z. Jiang, B. Krishnamachari, X. Zheng, S. Zhou, and Z. Niu, "Timely status update in wireless uplinks: Analytical solutions with asymptotic optimality," *IEEE Internet of Things Journal*, vol. 6, no. 2, pp. 3885–3898, 2019.
- [30] I. Kadota, A. Sinha, and E. Modiano, "Scheduling algorithms for optimizing age of information in wireless networks with throughput constraints," *IEEE/ACM Transactions on Networking*, vol. 27, no. 4, pp. 1359–1372, 2019.
- [31] A. Maatouk, M. Assaad, and A. Ephremides, "Minimizing the age of information: Noma or oma?" in *Proc. IEEE INFOCOM Workshops*, April 2019.
- [32] R. Yates and S. Kaul, "Status updates over unreliable multiaccess channels," in *Proc. IEEE ISIT*, June 2017.
- [33] R. Talak, S. Karaman, and E. Modiano, "Distributed scheduling algorithms for optimizing information freshness in wireless networks," in *Proc. IEEE SPAWC*, June 2018.
- [34] X. Chen, K. Gatsis, H. Hassani, and S. Bidokhti, "Age of Information in Random Access Channels," in *Proc. IEEE ISIT*, 2020.
- [35] R. Yates and S. Kaul, "Age of Information in Uncoordinated Unslotted Updating," in *Proc. IEEE ISIT*, 2020.
- [36] A. Maatouk, M. Assaad, and A. Ephremides, "On the age of information in a CSMA environment," *IEEE/ACM Transactions on Networking*, 2020.
- [37] A. Munari and A. Frolov, "Average Age of Information of Irregular Repetition Slotted ALOHA," 2020. [Online]. Available: <http://arxiv.org/abs/2004.01998>
- [38] M. Costa, M. Codreanu, and A. Ephremides, "Age of information with packet management," in *Proc. IEEE Int. Symposium on Inf. Th.*, 2014.
- [39] E. Sandgren, A. Graell i Amat, and F. Brännström, "On Frame Asynchronous Coded Slotted ALOHA: Asymptotic, Finite Length, and Delay Analysis," *IEEE Trans. Commun.*, vol. 65, no. 2, pp. 691–703, 2017.
- [40] A. Graell i Amat and G. Liva, "Finite-length analysis of irregular repetition slotted aloha in the waterfall region," *IEEE Commun. Letters*, vol. 22, no. 5, pp. 886–889, 2018.
- [41] A. Amraoui, A. Montanari, T. Richardson, and R. Urbanke, "Finite-length scaling for iteratively decoded LDPC ensembles," *IEEE Trans. Inf. Theory*, vol. 55, no. 2, pp. 473–498, 2009.
- [42] R. Gallager, *Stochastic Processes: Theory for Applications*. Cambridge University Press, 201.
- [43] E. Najm and E. Telatar, "Status updates in a multi-stream M/G/1/1 preemptive queue," in *Proc. IEEE INFOCOM Workshops*, 2018.
- [44] R. Devassy, G. Durisi, G. C. Ferrante, O. Simeone, and E. Uysal, "Reliable transmission of short packets through queues and noisy channels under latency and peak-age violation guarantees," *IEEE J. Sel. Areas Commun.*, vol. 37, no. 4, pp. 721–734, April 2019.
- [45] F. Chiariotti, O. Vikhrova, B. Soret, and P. Popovski, "Peak age of information distribution in tandem queue systems," *IEEE Comm. Letters*, 2020.
- [46] A. Glebov, N. Matveev, K. Andreev, A. Frolov, and A. Turlikov, "Achievability bounds for T-fold irregular repetition slotted aloha scheme in the Gaussian MAC," in *Proc. IEEE WCNC*, 2019.